JOURNAL OF MATERIALS SCIENCE 20 (1985) 2614–2622

The mechanism of the peak in strength and toughness at elevated temperatures in alumina containing a glass phase

C. R. CHEESEMAN, G. W. GROVES
Department of Metallurgy and Science of Materials, Oxford University, Oxford, UK

The fracture of an alumina containing 5% by volume of glass phase has been studied over the temperature range 20 to 900° C. Peaks in fracture stress and K_{Ic} at elevated temperatures have been confirmed to arise from softening of the glass phase by determining the temperature dependence of the viscosity of a glass of identical composition to that occurring in the ceramic. Observations of fracture surface show glass protrusions at temperatures of the peak in strength or K_{Ic} indicating the viscous stretching of glass particles bridging the opposite crack surfaces and a simple model considering the energy dissipated in this process is presented. The peaks in strength and K_{Ic} arise from this energy dissipation rather than from blunting of the crack.

1. Introduction

Many ceramics contain a glass phase resulting from incomplete crystallization of a glass or originating from a liquid present at high temperatures which assists in the compaction of the material. In some of these, for example a lithium disilicate glass–ceramic [1], hot pressed silicon nitride [2] and aluminas [3–7], a marked increase in strength or apparent toughness in fixed strain rate tests occurs at a temperature at which the glass might be expected to start to soften. In accordance with this, the temperature of the peak strength increases as the imposed strain rate increases. Although it appears to be agreed that the peak in strength is associated with the softening of the glass phase, the exact mechanism of the effect is less certain. The increase in strength has sometimes been ascribed to crack blunting. Thus, Davidge and Evans [8] suggested that "the peak is associated with viscous flow in the glass silicate phase. Near the peak temperature the plastic flow leads to crack blunting . . . ". Meredith *et al.* [4] also suggested the blunting of critical flaws as a mechanism and accounted for the greater strength increase of material containing a larger volume fraction of glass by an increase in the severity of blunting. However, Davidge and Tappin [3] noted that in an alumina the high strength could not be retained on cooling to room temperature, indicating a dynamic effect which they associated with both energy absorption and stress relief due to plasticity in the glass phase. Somewhat contrary to this, McClaren and Davidge [9] reported small statistical increases in strength in an alumina held at elevated temperature under stress and then tested at room temperature. Dalgleish *et al.* [6] found a peak in apparent toughness to be associated with grain-boundary flow in a glassy phase in aluminas and noted that sub-critical crack growth occurred in specimens of increased apparent toughness. Claussen *et al.* [5] spoke of the glass phase appearing to act as a tough glue under conditions of peak apparent toughness. The mechanics of sub-critical crack growth in aluminas was studied by Pabst *et al.* [7], who attributed the peak in apparent toughness and the associated crack growth to softening of the glass phase leading to grain-boundary sliding, crack branching and secondary cracking. A theoretical model given by Tsai and Raj [10] for a glass-containing ceramic focused attention on a damage zone ahead of a crack tip consisting of microcracks originating from cavities within the glass phase at triple grain junctions. If a large microcracked zone formed

0022–2461/85 $03.00 + .12

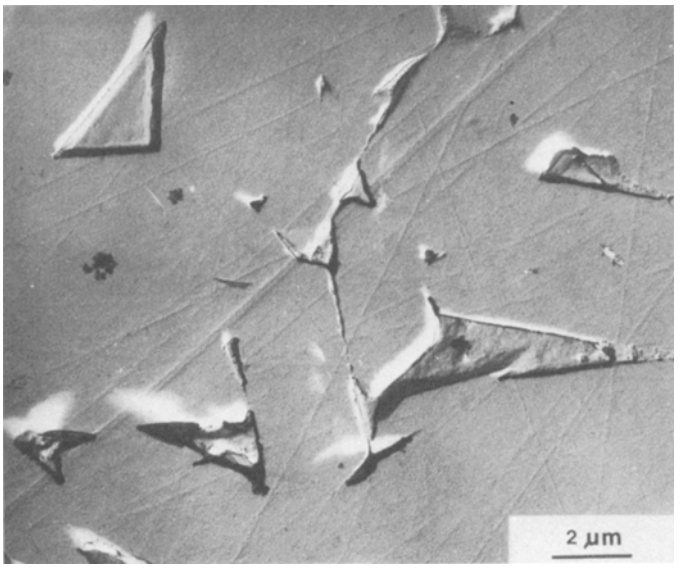

Figure 1 Particles of glass phase at grain-boundary junctions revealed by replication of etched surface.

during the time of the test, this could lead to slow crack growth and low strength, while a small damaged zone would be associated with a higher apparent strength.

In this paper we explore in detail the mechanism of the strength and apparent toughness peak in an alumina containing approximately 5% by volume of glass phase.

2. Experimental details

The material investigated was a commercially available 95% alumina. The microstructure was studied by optical observation of polished sections which were thermally etched at 1400° C for 30 min. In addition, to clearly reveal the glass phase polished sections were etched in a solution of 1% EDTA, 5% NaOH and 94% H_2O at 93° C, to cause preferential dissolution of the glassy phase. These surfaces were then replicated by a standard two-stage technique producing Au/Pd-shadowed carbon replicas which were examined by TEM (transmission electron microscopy). Specimens for direct TEM observation were also prepared, by ion-beam thinning. Compositional analysis of the material was carried out on a Camebax electron microprobe analyser, using wavelength dispersive analysis.

Measurements of strength and fracture toughness were carried out on bend specimens. Specimens were sliced out of blocks with a slow-speed diamond saw to dimensions 1.6 mm × 6 mm × 25 mm. For fracture toughness measurement the beams were given single edge cracks. Sharp cracks were initiated by pressing a diamond wedge into the edge of the specimen, following the technique developed by Almond and Roebuck [11]. These cracks were then grown by controlled three-point bending, using ink penetration to make the cracks observable and assist in control of their growth, which was probably by a stress-corrosion mechanism. A depth of at least 0.1 mm was ground from the indented surface since failure to do this can lead to anomalously low fracture toughness values [11, 12]. Specimens were located in a simple tube furnace for tests at elevated temperatures. Fracture surfaces were examined in a JEOL 35X SEM after coating with Au/Pd, and in some cases by carbon replicas viewed in the TEM.

3. Results and discussion

3.1. Microstructure and glass phase composition

The alumina, as-received, had an average grain size ~ 3 μm with some grains as large as 35 μm. It contained angular regions of glass as shown in Fig. 1. Confirmation that regions such as those shown in Fig. 1 were glassy was obtained by electron diffraction in the TEM. To obtain regions of glass large enough for electron microprobe analysis, the microstructure was coarsened by heat treating at 1550° C for 50 h (Fig. 2). The glass particles in the heat treated material were estimated to be sufficiently large at ~ 10 μm diameter to analyse with an incident electron energy of 10 keV without interference from surrounding matrix. Consistent results were obtained for particles analysed, supporting the validity of the analysis. In terms of

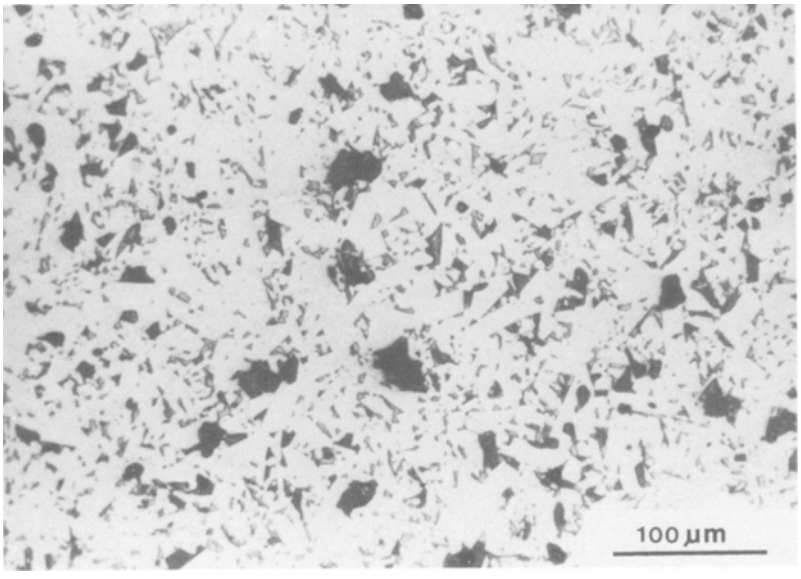

Figure 2 Optical micrograph of chemically etched surface of heat-treated specimen showing glass regions (grey areas).

weight percentage of the oxides present, the glass composition was found to be 35.3% Al_2O_3, 33.5% SiO_2, 27.0% CaO and 4.1% Na_2O. An energy dispersive analysis indicated that the above oxides were the major components of the glass.

3.2. Viscosity in the glass phase

In order to determine the temperature dependence of the viscosity of the glass phase, a glass of the composition determined by analysis, as given above, was made up by fusing the mixed oxides in a platinum crucible at 1550° C and rapidly cooling by pouring into a mould. Specimens for bend testing were sawn from the glass block and load relaxation was measured at four temperatures in the range 753 to 787° C. Assuming each fibre of the bent specimen behaves as a Maxwell solid (spring and viscous dashpot in series), it can be shown [12] that the load, L, on a three-point bend specimen held at fixed deflection falls off with time, t, according to the equation.

$$\ln L = -\frac{Et}{3\eta} + A \qquad (1)$$

where A is a constant depending on the specimen dimensions, E is the Young's modulus and η the viscosity of the glass. From the slopes of plots of $\ln L$ against t the values of $E/3\eta$ could be obtained and the plot of $\ln E/3\eta$ against $1/T$ is shown in Fig. 3. The slope of the line in Fig. 3 gives the activation energy governing viscous flow in the glass at $550 \pm 30\,\mathrm{kJ\,mol^{-1}}$, over the temperature range 753 to 787° C (the temperature dependence of the Young's modulus can be considered negligible over this temperature range).

3.3. The strength and toughness peak

The variation of strength, measured in three-point bending, with temperature is shown in Fig. 4. The peaks in apparent K_{Ic} determined from precracked specimens for two strain rates are shown in Fig. 5. The value of K_{Ic} at room temperature was determined to be $6.0 \pm 0.5\,\mathrm{MN\,m^{-3/2}}$. The peak in apparent K_{Ic}, therefore, represents an increase of some 50%, of the same order as the relative increase in fracture stress.

The values of apparent K_{Ic} shown in Fig. 5 were calculated from the maximum load, W, and the initial crack length, c, from the equation for a single edge cracked bend specimen

$$K_{Ic} = \frac{3YWlc^{1/2}}{2bd^2} \qquad (2)$$

where l is the distance between the outer loading points (23 mm) d is the specimen depth (6 mm) and b is the specimen width (1.6 mm). The factor Y has been determined by Brown and Srawley [13]. There was, however, a noticeable departure from linearity in the load–deflection curve for specimens tested at the temperature of the peak and above, indicating the occurrence of slow crack growth. This was also indicated by the delayed

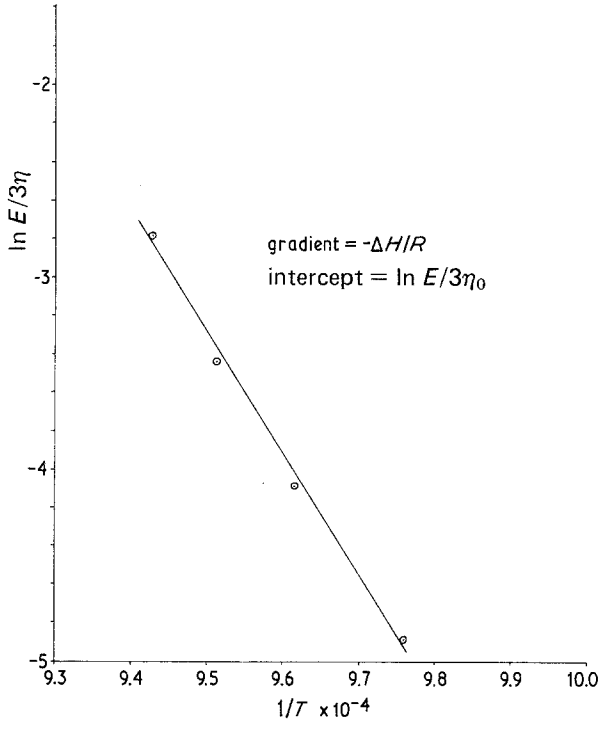

Figure 3 Graph of $\ln E/3\eta$ against $1/T$ for the integranular glass.

fracture of specimens subject to sustained stress intensity factors near K_{IC}. A treatment of the results taking into account this slow crack growth is given in a later section.

Specimens held at a stress intensity of 3 MN $m^{-3/2}$ for periods up to 30 min did not show any strengthening effect when the specimens were cooled and tested at room temperature. This indicates that crack blunting had not occurred during the period under load at elevated temperature.

The approximate temperature of the peak in strength or toughness can be predicted if it is assumed that it corresponds to the temperature at which the fracture mode of the glass changes from brittle to ductile. According to McClintock and Argon [14] the fracture transition temperature for a viscoelastic material is the temperature at which the time constant of loading Δt becomes comparable to the relaxation time, i.e. for a viscoelastic material tested in tension, the temperature at which

$$\Delta t \sim 3\eta/E \qquad (3)$$

From Fig. 3, the value of $1/T$ corresponding to the time Δt which is approximately 30 sec for a test carried out at a crosshead speed of 0.05 mm min^{-1} is $9.52 \times 10^{-4}\ K^{-1}$, corresponding to a

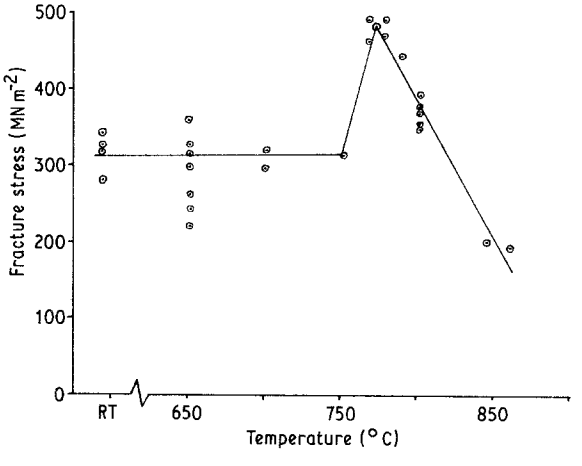

Figure 4 Variation of fracture stress with temperature for unnotched specimens.

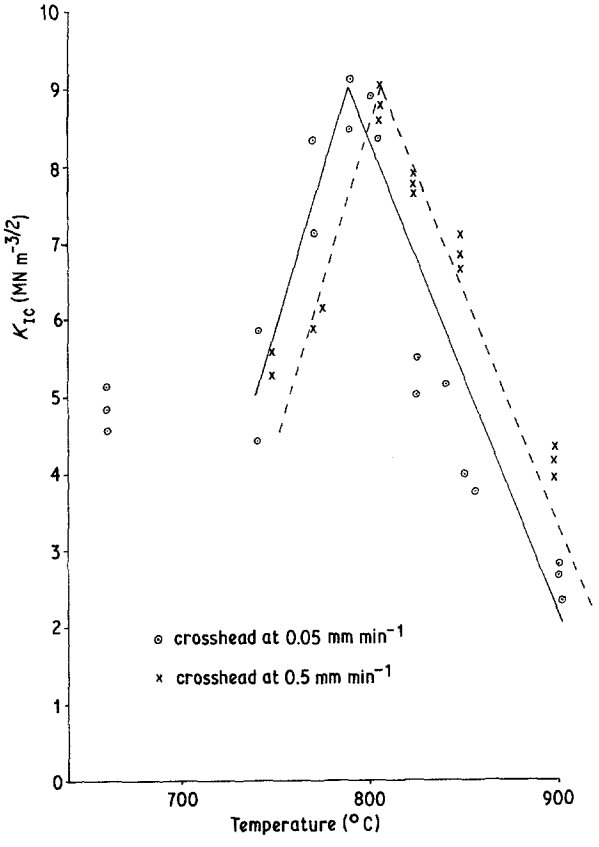

Figure 5 Variation of fracture toughness with temperture at two different loading rates.

peak temperature of 777° C, in good agreement with the results shown in Fig. 5. For a Δt of 3 sec, corresponding to the tests carried out at a crosshead speed of 0.5 mm min^{-1} the peak temperature predicted from an extrapolation of Fig. 3 is 816° C. The difference between the peak temperatures at the two strain rates as predicted, ~ 40° C, is somewhat larger than the difference shown in Fig. 5, but from the scatter of the data points in Fig. 5 the discrepancy appears to be within experimental error. Having regard to this experimental scatter and the approximate nature of Equation 3 the agreement between predicted and observed peak toughness temperatures is considered to be very satisfactory and strongly supportive of the proposition of previous authors [3–7] that the peak in toughness occurs at the ductile–brittle transition temperature of the glass phase.

3.4. Fractography

3.4.1. Specimen fractured below the peak temperature

The fracture surface was mainly intergranular, with a few regions showing cleavage steps indicative of regions of transgranular fracture (Fig. 6).

3.4.2. Specimens fractured at the toughness peak

These specimens showed intergranular fracture with a zone ahead of the precracked surface which was covered with a network of glassy ridges (Fig. 7a). Somewhat similar networks have been reported by Claussen *et al.* [5], and by Kromp and Pabst [15]. As the fracture surface was scanned along the direction of crack propagation the network disappeared and the fracture surface resumed the appearance characteristic of a low-temperature test. The exact dimensions of the network zone were difficult to measure as a sharp change in surface appearance did not occur. The morphology of the network suggests that the triple grain junction glassy phase is being pulled out of its intergranular sites into ridges during the separation of the fracture surfaces. There appears to be a direct link between the network zone ahead of the pre-existing crack, the nonlinearity of the load–deflection curves prior to fracture and the increased apparent toughness.

3.4.3. Specimens fractured at temperatures above peak in toughness

In the region of falling toughness above the tem-

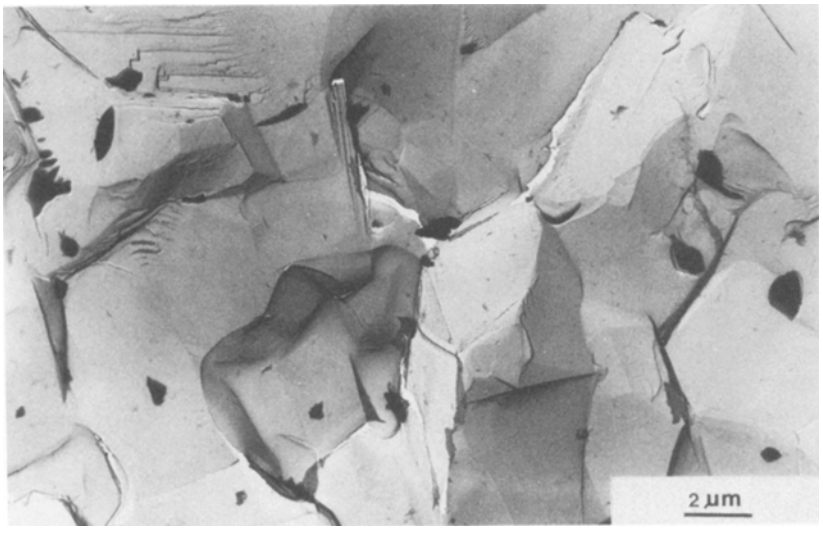

Figure 6 Carbon replica of low-temperature fracture surface.

perature of the peak the most noticeable difference between the fracture surfaces and those at peak toughness was that the glass was no longer in a continuous network but tended to be more concentrated at network nodes (Fig. 7b). However, the region of protruding glass extended further across the fracture surface. In certain cases the glass could be seen to have pulled out into definite spikes (Fig. 7c). This indicates greater lateral flow of the glass over the fracture surface than at the peak temperature so that the glass is gathered together at nodes into fibres. At the highest temperatures no glass protruding from the fracture surface was detectable. This may be because of rapid viscous relaxation of the glass, now of low viscosity, back to a level surface after the passage of the crack. Consistent with the idea that the glass has flowed back to coat the surface after fracture was the less angular appearance of the grains on the fracture surface at the highest temperatures, as seen in Fig. 7d. The "glazed" appearance of high temperature fracture surfaces in a similar alumina has been reported by Dalgleish *et al.* [6].

The spectrum of fracture surfaces observed over the full range of temperatures clearly shows the transition in the behaviour of the intergranular glass from brittle to viscous to freely flowing as the temperature is raised through the toughness and peak beyond. During a fracture at the temperature of the peak the fracture of the glass undergoes a transition from viscous to brittle as the crack accelerates and imposes an increased loading rate on the glass. At higher temperatures the glass behaves in a viscous way across the entire fracture surface.

3.5. Slow crack growth and *R*-curve interpretation of the strength and toughness peak

The fracture surface observations suggest that at and above the temperature of the peak, the crack is bridged by viscously deforming glass phase particles as it initially grows. As the crack grows, the amount of glass linking the fracture surfaces increases and the energy required for crack growth, R, must increase as the amount of work being done in viscous deformation of the intergranular glass increases.

To support this view of the fracture process, experimental R-curves were determined by taking a series of identically notched specimens and loading at a crosshead speed of 0.05 mm min^{-1} until slow crack growth occurred. The crosshead was then reversed at a fast rate and the specimen examined to measure the crack length with the aid of a dye to reveal the crack more clearly. The load at crosshead reversal was used to calculate G, the elastic energy release rate from the equation

$$G = K_I^2/E \tag{4}$$

where K_I, was determined from the load and measured crack length by Equation 2. At crack propagation

$$G = R \tag{5}$$

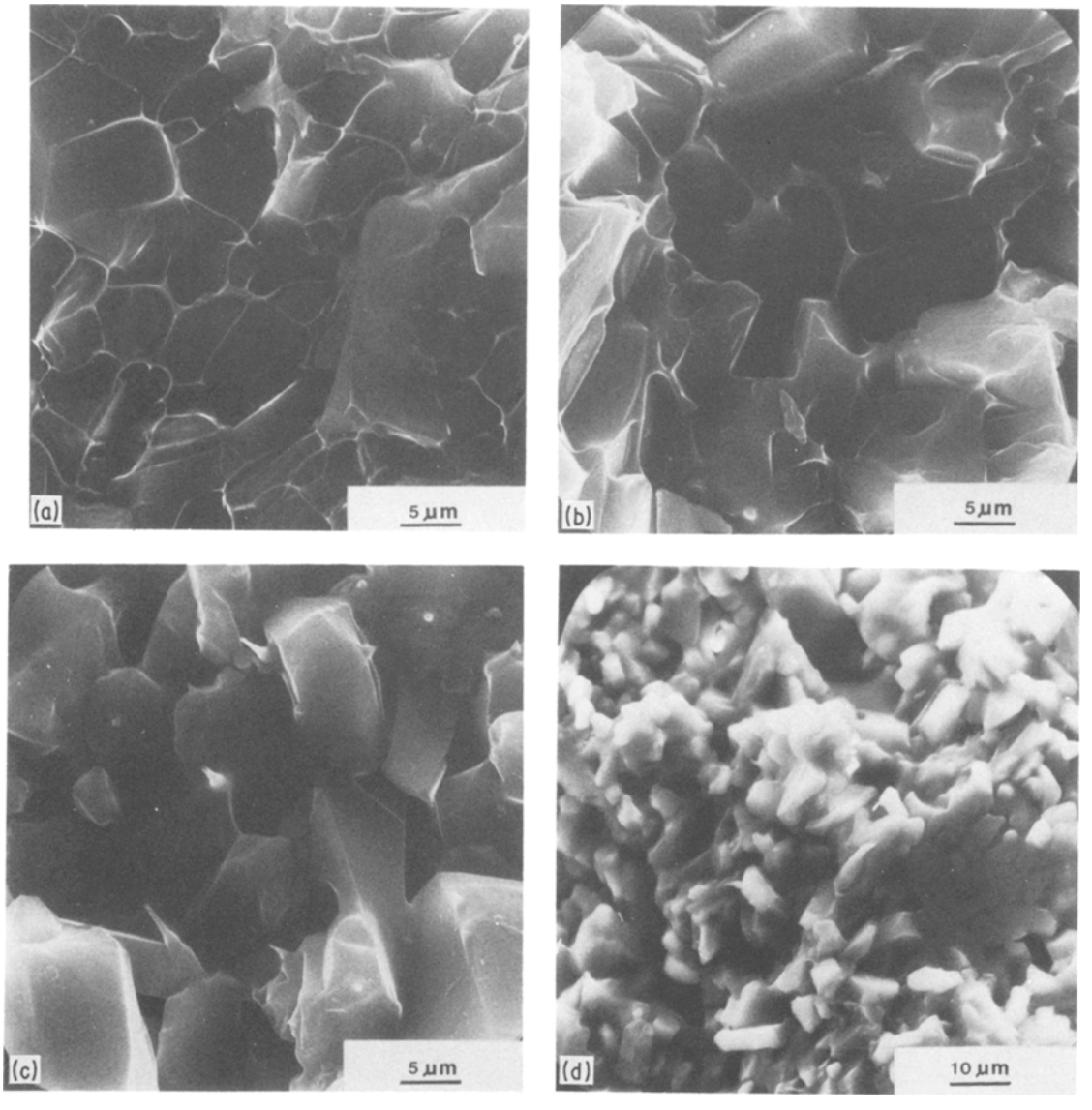

Figure 7 (a) Scanning electron micrograph showing glass network on notched specimen fractured at 800° C, 0.05 mm min^{-1}. (b) Fracture surface of notched specimen fractured at 825° C, 0.05 mm min^{-1}. (c) Fracture surface at notched specimen fractured at 850° C, 0.05 mm min^{-1}. (d) Fracture surface of notched specimen fractured at 900° C, 0.05 mm min^{-1}.

and the curves R against increase in crack length shown in Fig. 8 were obtained. The decrease in R with increasing temperature is very marked and is to be attributed primarily to the decrease in viscosity and, therefore, decreasing viscous work in deforming the glass regions.

The mechanics of crack growth for a given R-curve [16] are outlined in Fig. 9. The value of R_{max} represents the work done when the crack is growing with a steady-state region of deforming glass bridges maintaining a constant region behind the crack tip. In Fig. 9 the lines labelled σ_1, σ_2 and σ_3 represent the increases in elastic energy release rate with crack length (shown as linear merely for simplicity) for three applied stresses σ_1, σ_2 and σ_3, increasing in that order. Between σ_2 and σ_3 slow crack growth occurs and the load–deflection line departs from linearity. At σ_3 the crack growth becomes unstable since the energy release increases faster than the energy requirement. As the crack then accelerates the fracture mode of the glass can be expected to change from ductile

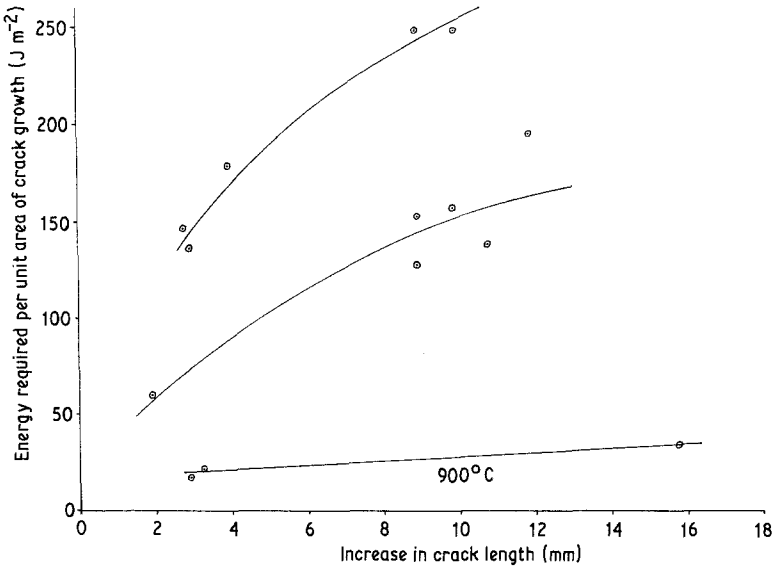

Figure 8 Experimental R-curves for specimens fractured at various temperatures.

to brittle. The sections of the R-curves shown in Fig. 8 lie between σ_2 and σ_3. The fact that the zone of glass ridges visible on the fracture surface is longer at 830° C than at 800° C is readily accounted for by consideration of Figs. 8 and 9.

In a specimen which is not pre-cracked, an inherent flaw can be considered to grow and acquire bridging glass particles, the increasing energy requirement demanding an increasing load until crack propagation finally becomes unstable.

Although R-curves, as shown in Fig. 8, describe the increasing energy requirement for crack growth under a given set of conditions, great care must be taken to distinguish them from R-curves describing slow crack growth under plane stress conditions in metals. In the latter case the crack growth is stable in the early stages in the sense that further growth always requires an increase in load. This is not the case in the alumina except under conditions of constant imposed strain rate. Under static con-

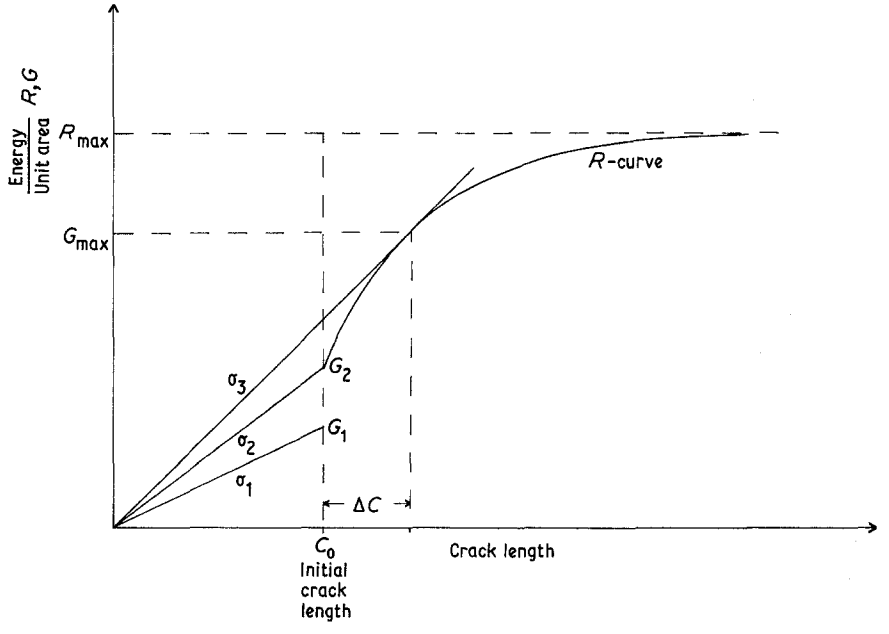

Figure 9 Schematic R-curve resulting in slow crack growth from a length C_0 to $C_0 + \Delta C$.

ditions the crack in alumina will continue to propagate to failure without further load increase. The strength and apparent toughness increases are purely dynamic effects.

A simple model can be constructed which indicates the factors governing the value of R_{max}. Particles of glass are considered to draw out as tensile specimens when the crack opens. The tensile stress required for each particle is given by

$$\sigma = 3\eta \mathrm{d}\epsilon/\mathrm{d}t \quad (6)$$

where 3η is the effective tensile viscosity and $\mathrm{d}\epsilon/\mathrm{d}t$ is the strain rate. The force F is then given by

$$F = \frac{3\eta A}{L}\frac{\mathrm{d}h}{\mathrm{d}t} \quad (7)$$

where L is the specimen length, A the area of cross-section and $\mathrm{d}h/\mathrm{d}t$ the rate of separation of the crack faces. If the volume $V = AL$ is constant

$$F = \frac{3V\eta}{L^2}\frac{\mathrm{d}h}{\mathrm{d}t} \quad (8)$$

and the work done in separating the glass completely is

$$W = 3\eta V \frac{\mathrm{d}h}{\mathrm{d}t}\int_{L_0}^{\infty}\frac{\mathrm{d}L}{L^2} \quad (9)$$

assuming $\mathrm{d}h/\mathrm{d}t$ to be constant. This gives

$$W = 3\eta A_0 \mathrm{d}h/\mathrm{d}t \quad (10)$$

where A_0 is the original cross sectional area of the particle.

Most of the work, W, is done in the early stages of deforming the particles so that the unrealistic upper limit of infinity in the integration does not greatly affect the model. Taking A_f to be the area fraction of glass initially present on the fracture surface

$$R_{max} \approx 3\eta A_f \mathrm{d}h/\mathrm{d}t \quad (11)$$

Equation 11 shows the dependence of the toughening limit on the viscosity and area fraction of glass, but the equation is difficult to apply quantitatively because of uncertainty as to the value of the crack surface separation rate which is presumably related to the crosshead speed but is not necessarily constant. At sufficient high values of $\mathrm{d}h/\mathrm{d}t$ or sufficiently low temperatures the glass would behave in a brittle way and Equation 11 would no longer be applicable.

4. Conclusions

The experiments and observations reported here confirm that the peak in strength and apparent toughness in constant strain rate tests found in alumina containing a glassy phase is due to viscous flow in the glass phase. The mechanism of the effect is not the blunting of cracks by flow of the glass phase but is the energy dissipated in viscous extension of glass bridges which link the opposite surfaces of the crack as the crack grows.

Acknowledgements

Thanks are due to the SERC for the award of a Studentship (C.R.C) and to Dr R. W. Davidge for helpful discussions during the course of this work.

References

1. K. JAMES and K. H. G. ASHBEE, *Prog. Mater. Sci.* **21** (1980) 3.
2. S. H. KNICKERBOCKER, A. ZANGVIL and S. D. BROWN, *J. Amer. Ceram. Soc.* **67** (1984) 365.
3. R. W. DAVIDGE and G. TAPPIN, *Proc. Brit. Ceram. Soc.* **15** (1970) 47.
4. H. MEREDITH, C. W. A. NEWEY and P. L. PRATT, *ibid.* **20** (1972) 299.
5. N. CLAUSSEN, R. F. PABST and C. P. LAHMANN, *ibid.* **25** (1975) 139.
6. B. J. DALGLEISH, A. FAKHR, P. L. PRATT and R. D. RAWLINGS, *J. Mater. Sci.* **14** (1979) 2605.
7. R. F. PABST, K. KROMP and G. POPP, *Proc. Brit. Ceram. Soc.* **32** (1982) 89.
8. R. W. DAVIDGE and A. G. EVANS, *Mater. Sci. Eng.* **6** (1970) 281.
9. J. R. McCLAREN and R. W. DAVIDGE, *Proc. Brit. Ceram. Soc.* **25** (1975) 299.
10. R. C. TSAI and R. RAJ, *Acta Metall.* **30** (1982) 1043.
11. E. A. ALMOND and B. ROEBUCK, *J. Mater. Sci.* **13** (1978) 2063.
12. C. R. CHEESEMAN, DPhil thesis, Oxford University (1984).
13. W. F. BROWN and J. E. SRAWLEY, ASTM Special Technical Pubication 410 (American Society for Testing Materials, Philadelphia, 1967).
14. F. A. McCLINTOCK and A. S. ARGON, "Mechanical Behaviour of Materials" (Addison-Westley, Massachusetts, USA, 1966) p. 548.
15. K. KROMP and R. F. PABST, *Met. Sci.* **15** (1981) 125.
16. D. BROEK, "Elementary Engineering Fracture Mechanics" (Sijthoff and Noordhoff, The Netherlands, 1978) p. 122.

Received 21 August
and accepted 13 September 1984